Structural Conditions for Cesium Migration to Si(100) Surface Employing Electronic Structure Calculations

ARTICLE *in* THE JOURNAL OF PHYSICAL CHEMISTRY C · FEBRUARY 2014

Impact Factor: 4.77 · DOI: 10.1021/jp4071423

THE JOURNAL OF PHYSICAL CHEMISTRY C

Article

pubs.acs.org/JPCC

Structural Conditions for Cesium Migration to Si(100) Surface Employing Electronic Structure Calculations

Peter R. Barry,* Patrick Philipp, and Tom Wirtz

Science and Analysis of Materials Department, Centre de Recherche Public−Gabriel Lippmann, 41 Rue du Brill, L-4422 Belvaux, Luxembourg

ABSTRACT: The mechanisms of cesium migration inside of a Si structure and to the Si(100) surface are explained using first-principles atomic-level simulation. Static electronic structure calculations of Cs surface coverage on Si(100) and within Si bulk reveal that energetically Cs prefers to reside on the surface as opposed to within the Si bulk. The reconstruction of the Si surfaces along with charge transfer due to Cs surface coverage lead to characteristic lowering of the surface work function, thus following well-established literature models. Ab initio molecular dynamics simulation at 300 K involving interstitial incorporation of Cs in the Si subsurface at various concentrations show that, given certain configurations, Cs readily migrates to the Si(100) surface. Comparatively, Cs substitution of Si within the subsurface under similar conditions does not readily migrate to the surface but instead appears to compromise to a great extent the silicon structure. Exploratory simulations of Cs substitution of Si at elevated temperatures where the kinetics of migration is accelerated reveal a greater tendency of Cs to migrate to the Si(100). Detailed analysis and explanation of migration processes are given in the context of Cs coverage, configuration, and depth of incorporation within the subsurface.

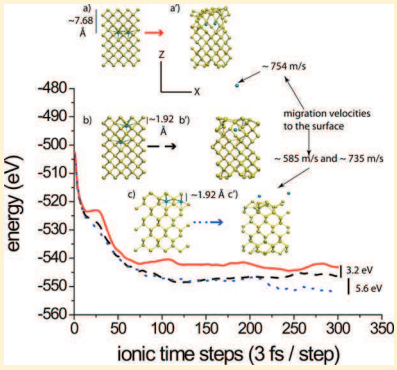

I. INTRODUCTION

Secondary ion mass spectrometry (SIMS) is an important technique used for the analysis of molecular, elemental, and isotopic compositions of trace elements, dopants, contaminants, and major elements in a variety of devices.[1−3] The main drawback of the technique is that the secondary ion yield depends heavily on the material environment which renders quantification extremely difficult.[4−6] In response, reactive primary ions such as oxygen[7−10] and cesium[11−13] are often utilized to increase the positive and negative secondary ion yield, respectively. In the case of metal and semiconductor samples where alkali primary ions such as cesium are often employed, the reduction of the sample's work function is frequently mentioned as the reason for the increase in negative secondary ion yield since it has been shown that negative ions' ionization probabilities scale exponentially with a lowering of the sample's work function.[14−17] The use of cesium also allows for quantification of secondary ion yields using the MCs_x^+ mode.[18,19]

The physical atomic mechanisms of sputtering of silicon by cesium ion bombardment in terms of the maintenance of a steady surface concentration in the presence of ion implantation, collision cascades, and eventual lowering of the sample's work function are not clearly understood. To the authors' knowledge, very little literature exists describing the physical migration mechanisms of relatively large alkali metals in silicon, while some exists for other species. Van de Wall[20] performed first-principles calculations for hydrogen interacting with bulk Si, the Si surface, and other impurities and defects in the Si lattice. His results show that hydrogen in the body-center cubic position in crystalline silicon maintains a relatively higher energy compared to that of H_2, H−P, and H−B in crystalline Si. More favorable energetically was Si−H at pre-existing isolated dangling bond sites and also Si−H on a pre-existing Si(111) surface. First-principle total-energy calculations of substitutional carbon incorporation at various concentrations into a hydrogenated Si(100) surface and subsurface sites also revealed a similar trend of increasing energy with depth of substitution beneath the surface.[21] In first-principles calculations of self-migration constants in silicon, Blöchl et al.[22] have shown that self-interstitial mechanisms dominate over other mechanisms. For cesium migration in silicon, Wittmaack[23] has suggested that implanted cesium atoms rapidly relocate to the receding surface in response to internal stress within the sample, thereby eventually passing through the solid−vacuum interface where they lose a valence electron and become bounded to the surface via dipole interactions.[24] In conclusion, however, it was acknowledged that the finer details of Cs atom transport to the surface, such as the time scale of the process, still need to be explained. The aim of this study is to specifically answer the question: does implanted Cs readily migrate to the Si(100) surface and if so under what physical conditions? A combination of electronic structure calculations and ab initio molecular dynamics (MD) simulations are employed to this end.

Received: July 18, 2013
Revised: December 30, 2013
Published: January 8, 2014

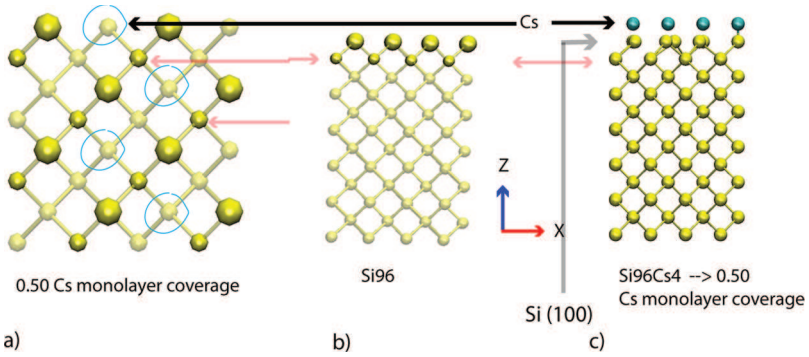

Figure 1. Cs surface coverage at 1/2 a monolayer on Si(100). (a) A top-down view on the Si(100) surfaces with the turquoise circles specifying the initial positions of Cs atoms 3.5−4 Å above the Si(100) surface. The enlarged, eight yellow opaque atoms (see (a) and (b)) are Si(100) atoms. The smaller, adjacent yellow opaque atoms are those of the adjacent layer within the surface. (b) A side view. (c) The identical initial positions of the Cs atoms at 1/2 monolayer coverage.

II. COMPUTATIONAL APPROACH AND DETAILS

The silicon diamond cubic structure (space group *Fd*3*m* at 25 °C, 1 atm)[25] is used as the initial starting structure. The unmodified silicon bulk and surfaces simulated in this study consist of 2 × 2 × 3 unit cells (i.e., 10.86 × 10.86 × 16.29 Å^3 for bulk and surfaces), resulting in 96 silicon atoms. Periodic boundary conditions are employed along the *x*, *y*, and *z* directions for the bulk systems, while for the surfaces, only the *x* and *y* directions are periodic with a vacuum of 15 Å in the *z*-direction, thus resulting in system dimensions of 10.86 × 10.86 × 31.29 Å^3. The interaction of cesium with the silicon (100) surface is probed by varying cesium surface coverage from zero (0) up to 1/2 a monolayer (see Figure 1) or four Cs atoms on a 2 × 2 unit surface cell also consisting of eight surface Si atoms. The Cs atoms are placed 3.5−4.0 Å above the unreconstructed Si(100) surface prior to simulation. Cs surface coverage is defined on a Si(100) surface atom percentage basis and is in agreement with work function changes as given in the literature where the function rises to that of a constant value (presumably to that of the pure metal) after demonstrating a minimum.[26] As described in Figure 1, the Cs atoms at varying surface coverage are placed on the Si(100) prior to surface reconstructions. Upon optimization, the Si(100) atoms as well as the deposited Cs atoms rearrange themselves to form dimers and to find the minimum energy configuration of Cs adsorption. In conjunction, up to three Cs atoms are incorporated into Si bulk and their formation energies calculated for comparison. The two groups of simulations previously described are cases of static, optimized electronic structure calculations with all converged atomic forces on the order of 10^{-3} eV/Å.

The calculations are performed within the framework of density functional theory (DFT) using the Vienna Ab Initio Simulation Package (VASP)[27−31] implementing the projector augmented-wave method.[32,33] The local density approximation (LDA)[34] in conjunction with the Ceperley−Alder (CA) form of the electron exchange-correlation is employed with an energy cutoff of 500 eV and 4 × 4 × 4 k-point mesh. The formation energies are determined by subtracting the energies of the optimized, converged reactant systems from the energies of the optimized, converged final, product systems while conserving the number of atoms for the reactants and products. For example, for a coverage of 0.125 monoloyer or one cesium atom on the Si(100) surface, the formation energy is calculated as follows

$$E_{\text{formation}} = E_{\text{Si-Cs}} - E_{\text{Si(100)}} - E_{\text{Cs}} \quad (1)$$

where $E_{\text{Si-Cs}}$ is the energy of the Si system with Cs adsorbed, $E_{\text{Si(100)}}$ the energy of the pristine p(2 × 2) Si(100) surface,[35] and E_{Cs} the energy of a Cs atom in vacuum. The atomic charges are determined using Bader charge analysis.[36,37] Lastly, ab initio molecular dynamics (MD) simulations are carried out to elucidate the dynamic process of migration where one to four Cs atoms are interstitially and substitutionally incorporated into the silicon subsurface within the NVT (i.e., constant number of atoms, constant volume, and constant temperature) ensemble at 300 K. A number of configurations are considered. A time step of 3 fs is employed.

III. RESULTS

To establish common ground with what has already been established in the literature, bond lengths and angles and lattice and elastic constants are calculated. Table 1 below gives these values as well as that of the literature. The calculation of the bulk Si−Si bond lengths, angles, and lattice constants is carried out while allowing the shape and size of the simulation box to change.

Table 1. Calculated Physical Properties of Pure Silicon

	Si−Si (Å)	Si−Si−Si (θ)	A_0 (Å)
LDA−CA (this work)	2.34	109.47	5.39
literature[a]	2.35	109.47	5.43
elastic constants (GPa)	C_{11}	C_{12}	C_{44}
LDA−CA (this work)	162.07	57.13	77.14
literature[a]	165.78	63.94	79.62

[a]Literature value.[25,38]

As is widely known, LDA tends to underestimate the bond lengths and lattice constant for a number of known material systems.[27] The calculated Si−Si bond length and lattice constant are nonetheless within 0.4 and 0.7%, respectively, of the literature values. In conjunction, the C_{11}, C_{12}, and C_{44} elastic constants agree reasonably well with the literature values with differences of 2, 11, and 3%, respectively. Furthermore, the typical dimer reconstruction on the Si(100) surface is obtained. The proposed buckled dimer configuration,[35] the lowest-energy configuration, is observed in our study as well. The dimer formations reduce the calculated surface energy by ∼1.91 eV, which is a 5% difference with the literature value of 2.02 eV.[35]

dx.doi.org/10.1021/jp4071423 | J. Phys. Chem. C 2014, 118, 3443−3450

The deposition of cesium on Si(100) influences the type of Si dimers formed. Figure 2 shows simulation snapshots of Cs

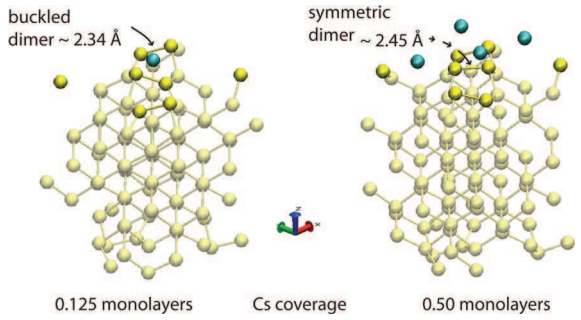

Figure 2. Cesium (turquoise) coverage of Si(100) (yellow, opague) at 0.125 and 0.50 monolayer surface coverage.

surface coverage of 0.125 and 0.50 monolayers. The dimer formation at Cs coverage of 0.125 monolayers resembles that of the pristine surface reconstruction or the buckled dimer configuration. At increased Cs coverage, however, toward that of 0.50 monolayers, some of the dimers change from a buckled configuration to one that is symmetric. This configuration is a higher-energy configuration[35] and demonstrates normally longer dimer bond lengths.

From Bader charge analysis, the atomic charge of each deposited Cs atom is determined after optimization of the structures. The cesium atoms prior to deposition exhibit a charge of approximately 0. Figure 3 illustrates the evolution in charge of the deposited Cs atoms on Si(100) upon optimization for each case of surface coverage. As explained previously, Cs surface coverage in terms of monolayers is determined as a percentage of the number of Si atoms on the Si(100) surface. For the system size utilized in this study, there are eight Si(100) atoms; thus, Cs surface coverage of 0.125 and 0.50 monolayers corresponds to one Cs atom and four Cs atoms, respectively, on Si(100). Given the large size of the deposited Cs atoms and the dynamic nature of the Cs adsorption optimization process in the presence of dimer reconstructions, the initial positions of both the Si(100) and the deposited Cs atoms change significantly. What this signifies is that the determined charge of the first deposited Cs atoms varies with surface coverage. The same phenomenon applies for the second deposited Cs atom in considering surface coverage of 0.25 monolayers and higher. As a result, it was deemed sensible to construct Figure 3 in arranging the Cs atomic charges, for each separate surface coverage, from high to low. As Figure 3 shows, at low surface coverage, the Cs atoms donate relatively more charge to the Si(100) surface, i.e., closer to 1 electron, whereas at higher surface coverage, relatively less charge is transferred to the surface on a per atom basis. Also, in considering the case of 1/2 a monolayer of Cs coverage, for example, one observes that each of the Cs atoms does not contribute an equal share of charge to the surface but instead progressively less.

The lowering of silicon's work function to a minimum followed by an increase to that of pure Cs upon complete surface coverage is a characteristic feature often cited in the literature studies for Cs coverage of Si. We first calculate a work function value of 4.85 eV for a pristine, reconstructed Si(100) surface which is in perfect agreement with literature value.[39] Figure 4 shows the decrease in Si(100) work function as a

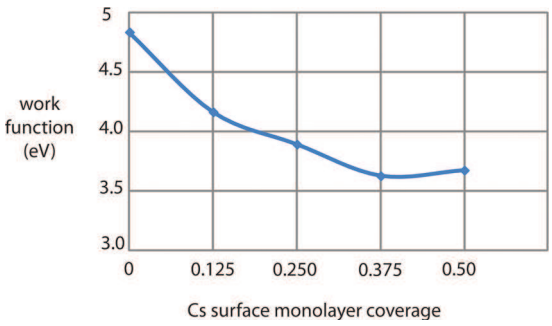

Figure 4. Work function as a result of Cs surface coverage from 0−0.5 monolayers. A calculated work function of 4.85 eV for a pristine Si(100) surface is in perfect agreement with the experimental literature value.[39]

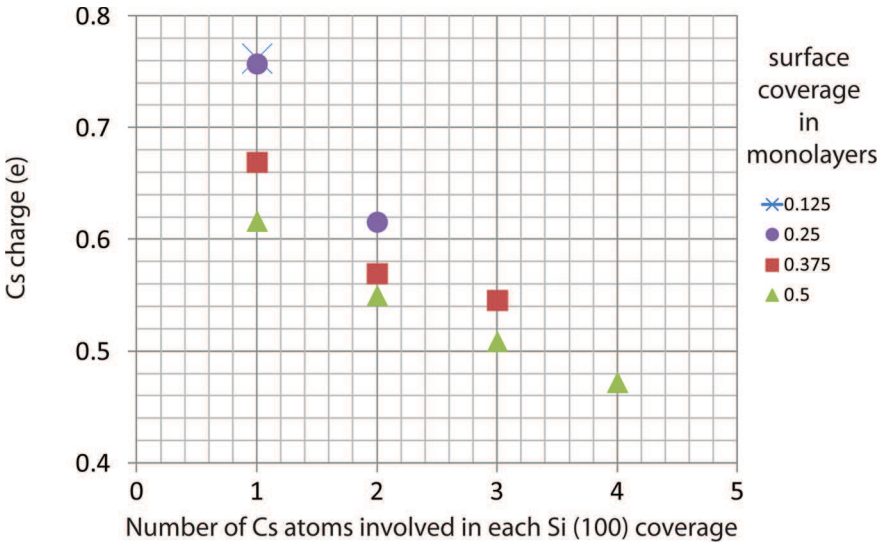

Figure 3. Deposited cesium atomic charge as a function of surface coverage. Cs surface coverage of 0.125 monolayer contains 1 Cs atom, 0.25 contains 2 Cs atoms, 0.375 contains 3 Cs atoms, and 1/2 monolayer contains 4 Cs atoms given our system size. All atoms in our DFT simulations start with a charge-neutral configuration.

dx.doi.org/10.1021/jp4071423 | J. Phys. Chem. C 2014, 118, 3443−3450

function of Cs surface coverage. Qualitatively consistent with the coverage of alkali metals on silicon, the Si work function decreases in characteristic fashion with increasing Cs coverage and reaches a minimum approximately in the range of 0.375–0.40 monolayer before increasing again presumably toward a constant value, i.e., that of the pure metal. Literature values vary somewhat depending on experimental conditions;[40] however, generally, saturation of Cs coverage on Si(100) is normally accepted to be at approximately 0.54 monolayer. Additionally, the minimum value of the work function in our simulation studies is in the rage of approximately 3.5–3.6 eV, whereas experimentally, the value is slightly inferior to 1.5 eV. Thus, in our simulation work, the experimental, qualitative work function trends are respected.

The formation energy of Cs incorporation into bulk silicon is compared to the formation energy for that of Cs deposited on Si(100). Figure 5 presents this comparison. The formation

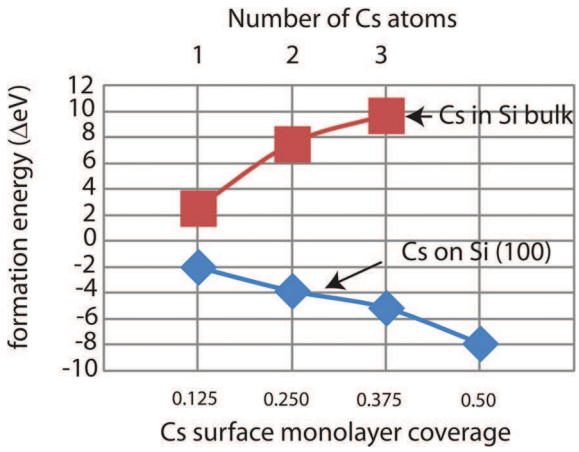

Figure 5. Energy of formation is given as a function of number of Cs atoms for two cases of Cs interaction with silicon (simulations performed at 0 K), i.e., Cs incorporated into bulk silicon (top axis) and cesium coverage of Si(100) (bottom axis) (see also Figure 1 for schematic of the latter).

energies are calculated according to eq 1. Figure 5 shows that the incorporation of Cs in bulk Si significantly raises the energy of the system by as much as 10 eV for three Cs atoms. This calculation was carried out at 0 K and at constant volume; thus, the shape of the structure was maintained albeit with severe internal deformation with three large Cs atoms incorporated. In comparison, adsorption of Cs on the Si(100) lowered the system's energy by approximately 6 eV in moving from a pristine reconstructed Si(100) to one with a Cs surface coverage of 1/2 monolayer. It is interesting to note the inflections in the graph of the formation energy in moving from 0.250 monolayer coverage to 0.375 and then on to 0.50. The shape of this graph resembles that of Figure 13 in ref 40 depicting that of the desorption energy as a function of surface coverage for Cs on a pristine Si(111).

To complement the series of static calculations which established clearly that Cs prefers to reside on the surface of silicon instead of within the structure, ab initio NVT (300 K) molecular dynamics simulations are performed to clarify the dynamic behaviors of Cs incorporation, at various concentrations and distributions within a silicon subsurface. In Figure 6, the evolution of system energy as a function of ionic time

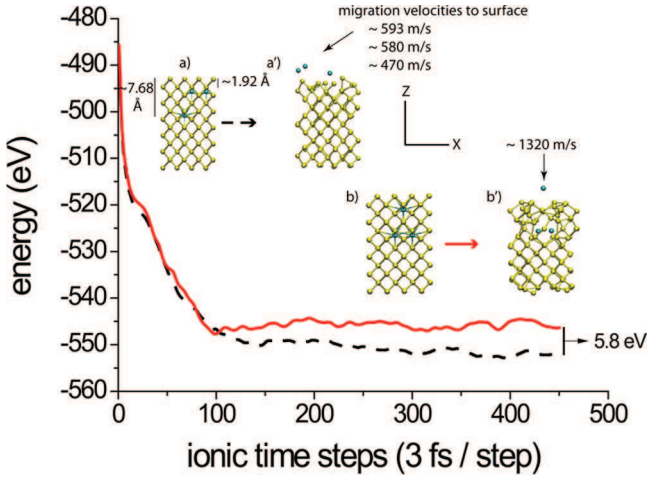

Figure 6. NVT ab initio molecular dynamics (300 K) plot of overall system energy as a function of ionic time steps. Three cesium atoms are incorporated into a silicon surface. Two comparable configurations (details given in the text) of cesium distribution in the surface are shown.

steps is given for two silicon surfaces, each incorporating three cesium atoms interstitially in the shallow, subsurface region.

In a simulation snapshot (Figure 6a), Cs is incorporated into the silicon surface without additional defects or loss of silicon. Two Cs atoms are placed at depths of ~1.92 Å beneath the Si(100) surface with one additional Cs placed at a depth of ~7.68 Å. The two topmost Cs atoms are ~3.84 Å apart, while their distances from the bottom-most cesium atom are 4.45 and 5.88 Å. In Figure 6b, the starting configuration is somewhat reversed compared to the previous. For this case, the distance between the topmost Cs atom and the two bottom-most Cs atoms is identical (~4.45 Å). The distance between the two bottom-most Cs atoms is ~3.84 Å. The relative distances beneath the Si(100) surface are the same as the previously mentioned case shown in the figure.

After approximately 1.4 ps of ab initio molecular dynamics simulations at 300 K, the differences between the two configurations of Cs in silicon are clearly visible. For the starting configuration in Figure 6a, the three cesium atoms migrate to and exit the Si(100) surface (see Figure 6a′). In describing the dynamic behavior as viewed from the ab initio molecular dynamics simulation snapshot, the topmost right cesium in Figure 6a′ starts to migrate straightway, in the z direction and toward the Si(100) surface. The leftmost top Cs atom migrates in the same direction albeit more slowly. Meanwhile, the bottom-most cesium in Figure 6a′ migrates rapidly toward the Si(100) surface as well and upon "feeling" the repulsion from the more slowly migrating topmost left cesium atom slows its migration speed and appears to stop, momentarily, in its new position with no apparent further displacement in the z direction. In response to the repulsion, the left topmost cesium accelerates its z direction migration and exits the Si(100) surface. While the topmost right cesium has already also exited the Si(100) surface, the bottom-most left cesium vibrates laterally in place for a few femtoseconds and then suddenly begins again to migrate along the path created by the previous topmost left cesium, which had already exited the Si(100) surface. The end configuration of this process is shown in Figure 6a′. Due to periodic boundary conditions within the plane of the Si(100) surface (i.e., along the x and y directions),

dx.doi.org/10.1021/jp4071423 | J. Phys. Chem. C 2014, 118, 3443–3450

two of the cesium atoms appear on the top left corner of Figure 6a′.

In moving from Figure 6b to 6b′, only one, the topmost cesium, atom migrates to and exits the Si(100) surface. The two bottom-most cesium atoms remain within the distorted structure during the duration of the simulation. The two bottom-most cesium atoms migrate simultaneously, at the same rate along the z direction toward the Si(100) surface and along the same path behind the exiting topmost cesium atom. After clearly migrating together along the same path toward the Si(100) surface, both atoms appear to repel each other laterally (along the $-x$ and x directions), thus, stopping their advancement in the z direction toward the Si(100) surface and finally remaining within the large resulting void created in the structure. The difference in the energy evolution shows that the silicon system prefers that the three cesium atoms migrate out of the structure. The energy difference between the two end configurations is approximately 5.8 eV. It is interesting to note that the migration of the lone Cs atom in Figure 6b′ is significantly faster than any of those depicted in Figure 6a′.

For the incorporation of two cesium atoms in a silicon surface, we consider Figure 7 where three cases are considered.

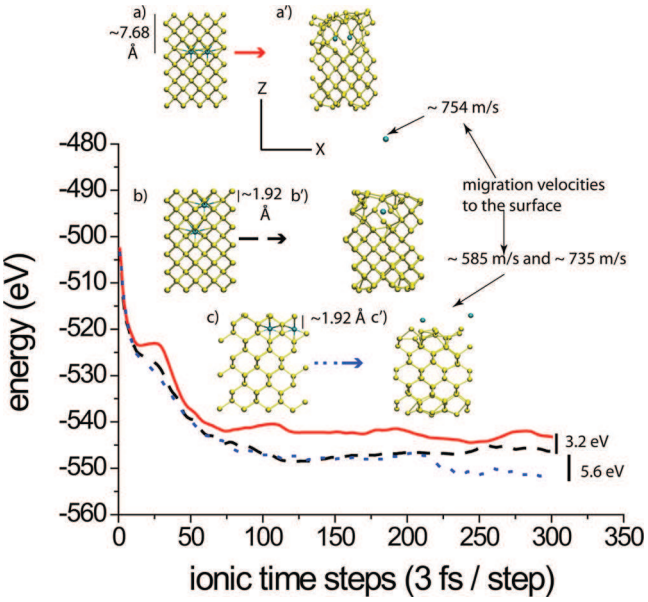

Figure 7. NVT ab initio molecular dynamics (300 K) plot of system energy as a function of ionic time steps. Two cesium atoms are incorporated into a silicon surface. Three comparable configurations (details given in the text) of cesium distribution in the surface are shown.

Figure 7a and 7a′ are almost a repeat of the simulation carried out in Figure 6b where two cesiums are interstitially placed at a distance of ∼7.68 Å beneath the Si(100) surface and ∼3.84 Å apart. Similarly, the starting simulation configuration depicted in Figure 7b is a copy of that for Figure 6a, minus the additional top rightmost cesium at a depth of ∼1.92 Å beneath the Si(100) surface. The last of the two-cesium simulations illustrated in Figure 7c is also a duplicate of Figure 6a, however, viewed from a different angle and minus the bottom-most cesium atom at a depth of ∼7.68 Å beneath the Si(100) surface.

Figure 7a′ shows the two cesium atoms which remain within the silicon surface. In response, the silicon atoms above the two cesium atoms appear to reconstruct in a noncrystalline manner, while a few silicon atoms beneath the two cesiums appear to have broken bonds. In Figure 7b′, the topmost cesium atom, initially at a depth of ∼1.92 Å, migrates out of the Si(100) surface; however, the bottom-most cesium, originally at ∼7.68 Å beneath the Si(100), remains in the structure just beneath the Si(100) surface in occupying the void partially created by the previously outmigrating cesium. Figures 7c and 7c′ demonstrate that two cesium atoms, placed interstitially at shallow depths of ∼1.92 Å beneath the Si(100) surface, prefer to readily migrate to and out of the surface. Similar to the simulations involving the three cesium atoms placed interstitially in a silicon surface, the evolution with ionic time steps of the simulations' energy favors the cases where the cesium atoms incorporated into the silicon structure migrate to and out of the surface (in this case Si(100)). For most of the cases where Cs migrates out of the structure, there appears to be no apparent significant difference in the migration velocities except for one of the aforementioned cases in Figure 6b.

Until now, the examples of cesium incorporated into a silicon surface involved the use of interstitial sites. In Table 2, a series of substitutional defects of silicon by cesium are considered in the context of ab initio NVT 300 K molecular dynamics simulation. A range of one to four cesium substitutions of silicon within the silicon surface at various depths and distribution beneath the Si(100) are considered. For all the cesium substitution silicon cases considered, only two show migration of cesium to the surface over the simulation time period considered.

In both of those cases, the cesium atom is substitutionally positioned only 1.92 Å beneath the Si(100) surface. In all the other cases, the structural integrity of the silicon surface in the region of cesium incorporation is completely compromised with very little migration of the cesium atoms. Figure 8 illustrates a few of these cases, some of which are listed in Table 2 and may be identified by the number of atoms and their depth of incorporation (see Table 2 caption). In Figure 8, the majority of the substitutional cesium within the silicon surface remains within the structure. According to the simulation snapshots, the surrounding silicon atoms significantly displace themselves, while the incorporated cesium atom reacts relatively slowly and fills the space vacated by the surrounding silicon atoms.

IV. ANALYSIS AND DISCUSSIONS

It is shown in Section III, based on various formation energies, that Cs readily resides on the silicon surface (100) as opposed to inside of the structure. With various ab initio MD simulations, it is also shown that under certain conditions Cs migrates, within a few picoseconds, from shallow, subsurface regions within the silicon structure to the Si(100) surface. First, a few thoughts on the former and then the latter.

Our findings regarding Cs coverage of Si(100) from the standpoint of charge transfer and resulting work function reduction are in agreement with the Langmuir−Gurney model.[24] According to this model, the discrete s-level of the free alkali metal atom (in this case cesium) broadens and shifts, thereby becoming partially emptied due to interactions with the substrate. The then partially charged adatom (i.e., cesium) consequently induces a negative screening charge density in the surface of the substrate, thus causing an adsorbate-induced dipole moment. In this way, one accounts for the lowering of the work function of pristine Si surfaces. Owing to the

dx.doi.org/10.1021/jp4071423 | J. Phys. Chem. C 2014, 118, 3443−3450

Table 2. Cesium Substitution of Silicon within a Silicon Surface at Varying Depths and Concentrations[a]

(a)		
system	depth (Å) beneath Si(100)	migration to the Si(100) surface
$Si_{95}Cs$	9.60	no
$Si_{95}Cs$	5.76	no
$Si_{95}Cs$	3.84	no
(b)		
system	depth (Å) beneath Si(100)	migration to Si(100) surface
$Si_{94}Cs_2$	9.60 (2 atoms)	no
$Si_{94}Cs_2$	5.76 (2 atoms)	no
$Si_{94}Cs_2$	3.84 (2 atoms)	no
(c)		
system	depth (Å) beneath Si(100)	migration to Si(100) surface
$Si_{93}Cs_3$	9.60	no
	9.60	no
	3.84	no
(d)		
system	depth (Å) beneath Si(100)	migration to Si(100) surface
$Si_{93}Cs_3$	9.60	no
	9.60	no
	5.76	no
(e)		
system	depth (Å) beneath Si(100)	migration to Si(100) surface
$Si_{93}Cs_3$	9.60	no
	9.60	no
	1.92	yes
(f)		
system	depth (Å) beneath Si(100)	migration to Si(100) surface
$Si_{92}Cs_4$	9.60	no
	9.60	no
	5.76	no
	1.92	yes

[a]Part a gives three separate cases of one Cs incorporation (see Figure 8, left column). Part b gives three separate cases of two Cs incorporation (see Figure 8, middle column). Parts c–e each show one case of three Cs's substitutionally incorporated within the silicon structure (see Figure 8, right column). Part f shows that for four Cs atoms incorporated into the silicon structure (no figure shown).

accumulation of adsorbate-induced dipoles, the interadsorbate interaction becomes largely repulsive, thus rendering a structure where the distances between adsorbates are maximized. Indeed, in this study, the Cs atomic distances increased with structural optimization and maintained interatomic distances in the range of 4–9 Å on Si(100). Furthermore, with increased absorbate coverage, the interadsorbate distances tend to decrease, thus increasing the electrostatic repulsion. To lower the total energy due to the increased repulsion with increased coverage, the model suggests that electrons flow back from the Fermi level of the substrate to the adsorbate (i.e., Cs). The evidence of this is the aforementioned reduction in positivity of the Cs charges (see Figure 3) with coverage and the increase of the work function after a minimum (Figure 4).

The overall trend observed for the change in work function as a function of surface coverage is in good agreement with experimental data found in the literature. However, the minimum work function value in the range of 3.5–3.6 eV obtained in this study is significantly higher than the experimental value of 1.2 eV reported for Cs adsorption.[40] With a pristine silicon surface work function of 4.83 eV, the maximum work function reduction in our study is −1.33 eV. During SIMS sputter experiments, this value ranges from −1.8[16] to −3.4 eV.[41] One source of error may be that the classical functionals in DFT calculations depend only on local electron density but take no dispersion effects into account which may be necessary in describing cesium.

According to the literature,[42] at 500 °C, the maximum solubility of Cs in solid Si at a density of 2.32 g/cm^3 is equivalent to a Cs atom fraction on the order of 10^{-8}. The incorporation of Cs in Si bulk presented in this study is on the order of 10^{-2} and thus is comparatively orders of magnitude higher. Nonetheless, given the current state of the art for simulations, our simulation results are interpreted within the limits of the local silicon environment of cesium incorporation. The ab-initio MD simulations for interstitial and substitutional cesium incorporation showed largely different behaviors. For cesium interstitial incorporation, cesium readily migrates, within a few picoseconds, to the Si(100) surface under conditions of relatively high, shallow cesium subsurface concentration. This hypothesis is supported by simulations depicted in Figures 6 and 7. In Figure 6a and 6a′, cesium incorporated at a depth of ∼7.68 Å beneath the Si(100) is able to migrate out of the structure probably because a high enough concentration of out-migrating cesium is present in the shallow subsurface region (at a depth of ∼1.92 Å) and opens up a migration pathway to the surface within the structure. In Figure 6b and 6b′, the two cesium atoms incorporated at a depth of ∼7.68 Å did not migrate out presumably because the pathway to the surface was not big enough as implied in the text in Section III. This hypothesis is further supported by the simulations of Figure 7. In Figure 7c and 7c′, the shallow, subsurface cesium atoms migrate out of the surface, while in Figure 7a and 7a′, without the aid of the presence of shallow, subsurface cesium atoms, more deeply incorporated cesium remains in the structure. In Figure 7b and 7b′, the concentration of shallow, subsurface cesium is presumably not high enough, hence the deeper implanted cesium remains in the structure in the large space vacated by the previous, out-migrating subsurface cesium.

For the case of cesium substitution of silicon within the silicon surface, migration of cesium to the surface and out of the silicon structure is a much rarer occurrence in comparison to cesium interstitial incorporation. Instead, in almost all cases considered, cesium simply distorts severely the silicon structure and displaces the surrounding silicon atoms with very little displacement or migration of the cesium atoms themselves. Much of this behavior is captured in Figure 8. There are two obvious points to immediately consider in this regard. The first one was mentioned before and involves the concentration of cesium in our simulations being well above the aforementioned solubility limit, thus leading to gross distortion or destruction of the structure. The second point has to do with the valence of cesium (+1) being different from that of silicon (+4). Due to the difference in valence, the incorporation of a large cesium in silicon inevitably weakens the silicon structure, especially in the case of substitution where four relatively stronger atomic silicon bonds are replaced by relatively weaker Cs–Si bonds. In spite of these findings at 300 K, it is very likely that at elevated temperature and thus enhanced kinetics substitutionally incorporated cesium in silicon would eventually migrate to the Si(100) surface under the right conditions of concentration and depth of implantation. Exploratory simulations for the

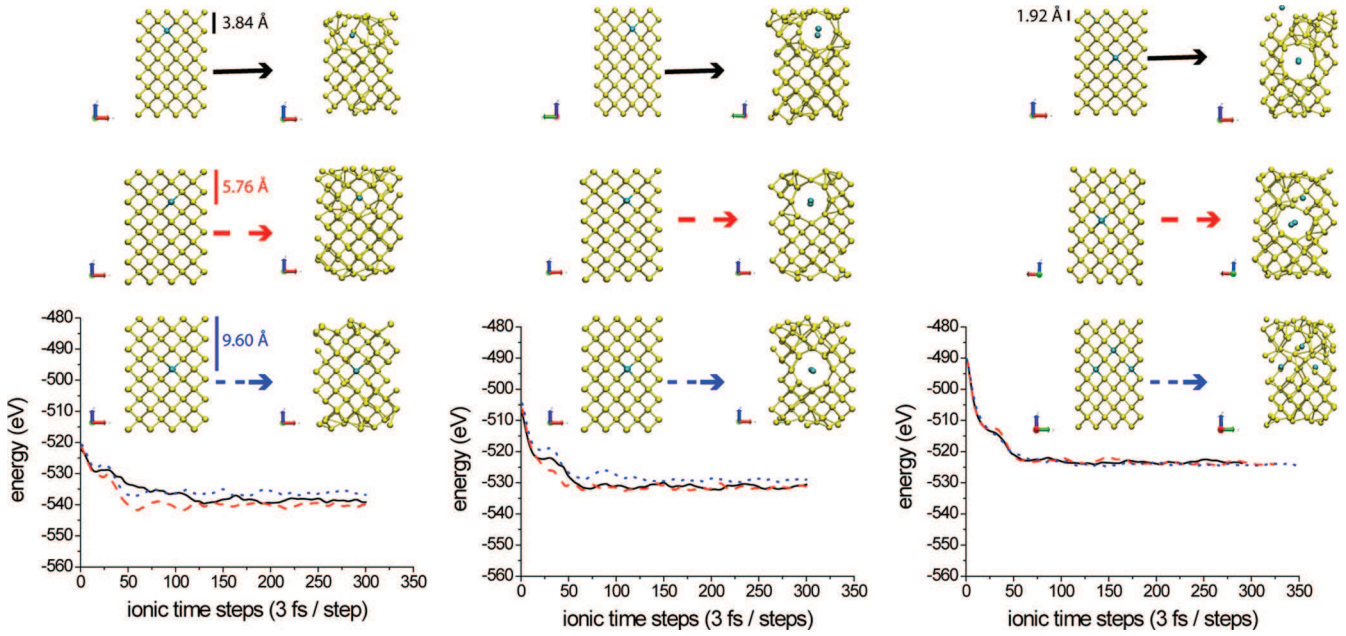

Figure 8. Comparisons of cesium substitution of silicon within the silicon surface at various cesium concentrations and distributions. The snapshot insets show visually the start and final configurations for the simulations and are color coded with the plots of the energy evolution. In moving from left to right, the snapshots in columns 1, 2, and 3 represent 1, 2, and 3 substitutional cesium incorporation, respectively. Each snapshot corresponds to entries in Table 2 (see text). The graphs show similar system energy evolution for given cesium incorporation regardless of implantation depth for cases where cesium does not migrate out of the structure.

structure shown in Figure 8, the topmost and leftmost column (with a single Cs incorporation at a depth of 3.84 Å beneath the surface), are carried out at temperatures of 500, 700, and 1000 K. At 500 K, the implanted cesium remains in the silicon structure as was the case at 300 K over the course of the simulation (on the order of 2 ps). At 700 K, however, the cesium atom migrates out of the silicon structure (migration velocity of ∼467 m/s) and did so even more readily at 1000 K (migration velocity of ∼599 m/s). Overall, these simulation conditions thus capture the essential conditions of SIMS ion bombardment and give some insights regarding the time scales and conditions under which Cs migrates to the silicon surface under the force of structural strain.

Finally, the effect of oxygen in and on the surface of silicon in the presence of cesium was not treated in this study. As is known from the literature,[43] absorption of oxygen to the silicon surface provides an attachment site for impinging cesium ions and thereby increases the retention capacity of cesium significantly. This allows for the establishment of a high concentration of chemically inert cesium on the surface, which affects adversely the negative ionization yield. It is surmised that oxygen within the shallow silicon subsurface region would add to the internal stress of the structure, thereby encouraging the migration and eventual expulsion of Cs. However, oxygen is readily incorporated into the silicon structure (i.e., inward migration), while that for cesium is out-going (against the migration direction of oxygen). Additionally, oxygen, being more electronegative than silicon, may more readily interact within the structure with reactive cesium at the expense of silicon. This may lead to Cs−O complexes being formed within the silicon structure as a separate phase. Indeed, a separate study of the role of oxygen on cesium migration in silicon would be needed to clarify the matter.

V. DRAWN CONCLUSIONS

From a charge transfer and change in work function perspective, Cs interacts with Si in a very similar manner to what has been observed experimentally. The qualitative and also semiquantitative agreement of our simulation results with experiment provides a reasonable basis for arguing that, energetically, cesium prefers to reside on the Si(100) surface as opposed to within the Si bulk. This suggests that Cs incorporated into a Si structure would show a tendency to migrate toward the Si surface. The case of Cs substitution of Si leads to significant structural degradation with relatively rare Cs migration events to the Si(100) surface over the simulation time scale considered (that is, a few picoseconds). Comparatively, interstitial placement of Cs in Si demonstrates a stronger tendency of Cs to migrate toward the Si(100) surface over the same simulation time scale. Such migration events are responses to physical stress induced by the large Cs atoms that exhibit relatively shallow Cs subsurface implantation depths (i.e., ∼7 Å or less) and relatively high subsurface concentration. It has long been established that Cs incorporation is known to enhance negative secondary ion emission in SIMS by lowering the work function of metallic and semiconductor samples. This work gives for the first time insight into the migration processes for Cs atoms inside Si and its adsorption on Si surfaces.

■ AUTHOR INFORMATION

Corresponding Author

*E-mail: barry@lippmann.lu.

Notes

The authors declare no competing financial interest.

■ ACKNOWLEDGMENTS

The present project is supported by the National Research Fund, Luxembourg, and cofunded by the Marie Curie Actions of the European Commission (FP7-COFUND).

■ REFERENCES

(1) Benninghoven, A. Chemical Analysis of Inorganic and Organic Surfaces and Thin Films by Static Time-of-Flight Secondary Ion Mass Spectrometry (TOF-SIMS). *Angew. Chem., Int. Ed. Engl.* **1994**, *33* (10), 1023−1043.
(2) Zalm, P. C. Ultra shallow doping profiling with SIMS. *Rep. Prog. Phys.* **1995**, *58*, 1321.
(3) Adriaens, A.; Van Vaeck, L.; Adams, F. Static secondary ion mass spectrometry (S-SIMS) Part 2: material science applications. *Mass Spectrom. Rev.* **1999**, *18* (1), 48−81.
(4) Pillatsch, L.; Wirtz, T.; Migeon, H. N.; Scherrer, H. SIMS using negative primary ion bombardment. *Surf. Interface Anal.* **2010**, *42* (6−7), 645−648.
(5) Gnaser, H. Sputtering of Cs-carrying diatomic cations from surfaces by keV Cs+ irradiation. *Int. J. Mass Spectrom.* **1998**, *174* (1−3), 119−127.
(6) van der Heide, P. A. W.; Azzarello, F. V. Work function, valence band and secondary ion intensity variations noted during the initial stages of SIMS depth profiling of Si and SiO2 by Cs+. *Surf. Sci.* **2003**, *531*, L369−L377.
(7) Alay, J. L.; Vandervorst, W. Model for the Emission of Si+ Ions During Oxygen Bombardment of Si(100) Surfaces. *Phys. Rev. B* **1994**, *50* (20), 15015−15025.
(8) Yu, M. L. Chemical Enhancement Effects in Sims Analysis. *Nucl. Instrum. Methods Phys. Res., Sect. B* **1986**, *15* (1−6), 151−158.
(9) Williams, P.; Evans, C. A. Anomalous Enhancement of Negative Sputtered Ion Emission by Oxygen. *Surf. Sci.* **1978**, *78* (2), 324−338.
(10) Serrano, J. J.; De Witte, H.; Vandervorst, W.; Guzman, B.; Blanco, J. M. Simulation of the initial transient of the Si+ and O+ signals from oxygen sputtered silicon by means of independent models on sputtering and secondary ionization. *J. Appl. Phys.* **2001**, *89* (9), 5191−5198.
(11) Wittmaack, K. Basic requirements for quantitative SIMS analysis using cesium bombardment and detection of MCs+ secondary ions. *Nucl. Instrum. Methods Phys. Res., Sect. B* **1992**, *64*, 621.
(12) van der Heide, P. A. W. Cesium-induced transient effects on the Si+ and Si- secondary ion emissions from Si and SiO2. *Surf. Sci.* **2000**, *447*, 62.
(13) Philipp, P.; Wirtz, T.; Migeon, H. N.; Scherrer, H. SIMS analysis with neutral cesium deposition: Negative secondary ion sensitivity increase and quantification aspects. *Int. J. Mass Spectrom.* **2006**, *253* (1−2), 71−78.
(14) Bernheim, M.; Bourse, F. L. On the velocity dependence for negative ionization of atoms sputtered from cesiated surfaces: an experimental study. *Nucl. Instrum. Methods Phys. Res., Sect. B* **1987**, *27*, 94.
(15) Gnaser, H. Exponential scaling of sputtered negative-ion yields with transient work-function changes on Cs+-bombarded surfaces. *Phys. Rev. B* **1996**, *54* (23), 16456.
(16) Philipp, P.; Wirtz, T.; Migeon, H. N.; Scherrer, H. Electron work function decrease in SIMS analysis induced by neutral cesium deposition. *Int. J. Mass Spectrom.* **2007**, *264* (1), 70−83.
(17) Wirtz, T.; Migeon, H. N. Work function shifts and variations of ionization probabilities occuring during SIMS analyses using an in situ deposition of Cs°. *Surf. Sci.* **2004**, *561*, 200−207.
(18) Wirtz, T.; Duez, B.; Migeon, H. N.; Scherrer, H. Useful yields of MCs+ and MCs2+ clusters: a comparative study between the Cameca IMS 4f and the Cation Mass Spectrometer. *Int. J. Mass Spectrom.* **2001**, *209*, 57.
(19) Gnaser, H. Correlations in Secondary-Ion Yields from Cs-Implanted Semiconductors. *Surf. Sci.* **1995**, *342* (1−3), 319−326.
(20) Vandewalle, C. G. Energies of Various Configurations of Hydrogen in Silicon. *Phys. Rev. B* **1994**, *49* (7), 4579−4585.
(21) Sonnet, P.; Selloni, A.; Stauffer, L.; De Vita, A.; Car, R. Energetics of substitutional carbon in hydrogenated Si(100). *Phys. Rev. B* **2002**, *65* (8).
(22) Blochl, P. E.; Smargiassi, E.; Car, R.; Laks, D. B.; Andreoni, W.; Pantelides, S. T. 1 St-Principles Calculations of Self-Diffusion Constants in Silicon. *Phys. Rev. Lett.* **1993**, *70* (16), 2435−2438.
(23) Wittmaack, K. Mechanisms responsible for inducing and balancing the presence of Cs adatoms in dynamic Cs based SIMS. *Int. J. Mass Spectrom.* **2012**, *313* (0), 68−72.
(24) Scheffler, M.; Stampfl, C. Theory of adsorption on metal substrates. In *Handbook of Surface Science: Electronic Structure*; Horn, K., Scheffler, M., Eds.; Elsevier: Amsterdam, 2000; Vol. 2, pp 286−356.
(25) Chemical Rubber Company (Cleveland; Ohio); Lide, D. R. *CRC handbook of chemistry and physics: 1994−1995; a ready-reference book of chemical and physical data*; CRC Press: Boca Raton u.a., 1994.
(26) Mausfriedrichs, W.; Dieckhoff, S.; Wehrhahn, M.; Kempter, V. Alkali Adsorption on W(110) Studied by Metastable Impact Electron-Spectroscopy. *Surf. Sci.* **1991**, *253* (1−3), 137−146.
(27) Mattsson, A. E.; Schultz, P. A.; Desjarlais, M. P.; Mattsson, T. R.; Leung, K. Designing meaningful density functional theory calculations in materials science - a primer. *Modell. Simul. Mater. Sci. Eng.* **2005**, *13* (1), R1−R31.
(28) Kresse, G.; Hafner, J. Abinitio Molecular-Dynamics for Liquid-Metals. *Phys. Rev. B* **1993**, *47* (1), 558−561.
(29) Kresse, G.; Hafner, J. Ab-Initio Molecular-Dynamics Simulation of the Liquid-Metal Amorphous-Semiconductor Transition in Germanium. *Phys. Rev. B* **1994**, *49* (20), 14251−14269.
(30) Kresse, G.; Furthmuller, J. Efficiency of ab-initio total energy calculations for metals and semiconductors using a plane-wave basis set. *Comput. Mater. Sci.* **1996**, *6* (1), 15−50.
(31) Kresse, G.; Furthmuller, J. Efficient iterative schemes for ab initio total-energy calculations using a plane-wave basis set. *Phys. Rev. B* **1996**, *54* (16), 11169−11186.
(32) Blochl, P. E. Projector Augmented-Wave Method. *Phys. Rev. B* **1994**, *50* (24), 17953−17979.
(33) Kresse, G.; Joubert, D. From ultrasoft pseudopotentials to the projector augmented-wave method. *Phys. Rev. B* **1999**, *59* (3), 1758−1775.
(34) Perdew, J. P.; Zunger, A. Self-Interaction Correction to Density-Functional Approximations for Many-Electron Systems. *Phys. Rev. B* **1981**, *23* (10), 5048−5079.
(35) Ramstad, A.; Brocks, G.; Kelly, P. J. Theoretical-Study of the Si(100) Surface Reconstruction. *Phys. Rev. B* **1995**, *51* (20), 14504−14523.
(36) Bader, R. F. W. A Quantum-Theory of Molecular-Structure and Its Applications. *Chem. Rev.* **1991**, *91* (5), 893−928.
(37) *Bader Charge Analysis*, 2013.
(38) Askeland, D. R.; Fulay, P. P. *The science and engineering of materials*, 4th ed.; Thomson Brooks/Cole: Pacific Grove, CA, 2003.
(39) Gnaser, H. Initial stages of cesium incorporation on keV-Cs +-irradiated surfaces: Positive-ion emission and work-function changes11. *Phys. Rev. B* **1996**, *54* (23), 17141.
(40) Wittmaack, K. Unravelling the secrets of Cs controlled secondary ion formation: Evidence of the dominance of site specific surface chemistry, alloying and ionic bonding. *Surf. Sci. Rep.* **2013**, *68* (1), 108−230.
(41) Brison, J.; Mine, N.; Poisseroux, S.; Douhard, B.; Vitchev, R. G.; Houssiau, L. Measurement and modeling of work function changes during low energy cesium sputtering. *Surf. Sci.* **2007**, *601* (6), 1467−1472.
(42) Sangster, J. Cs-Si (cesium-silicon) system. *J. Phase Equilib. Diffus.* **2006**, *27* (2), 188−189.
(43) Berghmans, B.; Vandervorst, W. The effect of oxygen during irradiation of silicon with low energy Cs+ ions. *J. Appl. Phys.* **2009**, *106* (3).